Determining the structural relaxation times deep in the glassy state of the pharmaceutical Telmisartan



2010 J. Phys.: Condens. Matter 22 125902

(http://iopscience.iop.org/0953-8984/22/12/125902)

J. Phys.: Condens. Matter **22** (2010) 125902 (11pp) doi:10.1088/0953-8984/22/12/125902

# Determining the structural relaxation times deep in the glassy state of the pharmaceutical Telmisartan

**K Adrjanowicz[1], M Paluch[1] and K L Ngai[2]**

[1] Institute of Physics, University of Silesia, Uniwersytecka 4, 40-007 Katowice, Poland
[2] Naval Research Laboratory, Washington, DC 20375-5320, USA

Received 18 January 2010, in final form 15 February 2010
Published 12 March 2010
Online at stacks.iop.org/JPhysCM/22/125902

**Abstract**

By using the dielectric relaxation method proposed recently by Casalini and Roland (2009 *Phys. Rev. Lett.* **102** 035701), we were able to determine the structural $\alpha$-relaxation times deep in the glassy state of the pharmaceutical, Telmisartan. Normally, deep in the glassy state $\tau_\alpha$ is so long that it cannot be measured but $\tau_\beta$, which is usually much shorter, can be directly determined. The method basically takes advantage of the connection between the $\alpha$-relaxation and the secondary $\beta$-relaxation of the Johari–Goldstein kind, including a relation between their relaxation times $\tau_\alpha$ and $\tau_\beta$, respectively. Thus, $\tau_\alpha$ of Telmisartan were determined by monitoring the change of the dielectric $\beta$-loss, $\varepsilon''$, with physical aging time at temperatures well below the vitrification temperature. The values of $\tau_\alpha$ were compared with those expected by the coupling model (CM). Unequivocal comparison cannot be made in the case of Telmisartan because its $\beta$-loss peak is extremely broad, and the CM predicts only an order of magnitude agreement between the primitive relaxation frequency and the $\beta$-peak frequency. We also made an attempt to analyze all isothermal and aging susceptibility data after transformation into the electric modulus representation. The $\tau_\alpha$ found in the glass state by using the method of Casalini and Roland in the modulus representation are similar to those obtained in the susceptibility representation. However, it is remarkable that the stretching parameter $\beta_{\mathrm{KWW}-M} = 0.51$ in the electric modulus representation gives more precise fits to the aging data than in the susceptibility representation with $\beta_{\mathrm{KWW}} = 0.61$. Our results suggest that the electric modulus representation may be useful as an alternative to analyze aging data, especially in the case of highly polar glassformers having a large ratio of low frequency and high frequency dielectric constants, such as the Telmisartan studied.

(Some figures in this article are in colour only in the electronic version)

## 1. Background of the method to determine the structural relaxation times deep in the glassy state

Direct determination of the structural $\alpha$-relaxation time $\tau_\alpha$ deep in the glassy state by standard experimental setup is not possible simply, because it is exceedingly long and far outside the time windows of conventional spectroscopy. Thus $\tau_\alpha$ is an unknown quantity at temperatures sufficiently lower than $T_g$. However, $\tau_\alpha$ together with the secondary relaxation time $\tau_\beta$ are relevant quantities characterizing molecular motions in glassy state that are important for the application of amorphous pharmaceuticals concerning storage condition and life time, as well as guarding against crystallization [1–6]. Hence, it is important to have some means to determine $\tau_\alpha$ deep in the glassy state. There is no problem in the case of $\tau_\beta$ because it is usually much shorter and can be directly determined at temperatures way below the vitrification temperature $T_g$; its change with physical aging can be monitored as well.

Recently Casalini and Roland (CR) [7] proposed a new method to determine $\tau_\alpha$ in the glassy state by exploiting the connection between the $\alpha$-relaxation and the secondary $\beta$-relaxation of the Johari–Goldstein type. CR demonstrated for an amorphous polymer, poly(vinylethylene), that the observed change of the $\beta$-relaxation with physical aging can be used to deduce the structural relaxation dynamics below $T_g$. They measured the variation of the imaginary part of dielectric

 

permittivity $\varepsilon''(\tilde{f}, t_{ag})$ of PVE with aging time $t_{ag}$ at fixed frequency $\tilde{f}$, which can be successfully described by the following equation

$$\frac{\varepsilon''(\tilde{f}, t_{ag})}{\varepsilon''(\tilde{f}, t_{ag=0})} = \left\{ \Delta\varepsilon''(\tilde{f}, t_{ag}) \times \exp\left[ -\frac{t_{ag}}{\tau_{ag}} \right]^{\beta_{ag}} + \varepsilon''_{eq}(\tilde{f}) \right\} \Big/ \varepsilon''(\tilde{f}, t_{ag=0}), \quad (1)$$

where $\varepsilon''_{eq}(\tilde{f}) \equiv \varepsilon''(\tilde{f}, t_{ag} \to \infty)$ is an equilibrium value, $\Delta\varepsilon''(\tilde{f}, t_{ag}) = \varepsilon''(\tilde{f}, t_{ag} = 0) - \varepsilon''_{eq}$ is the change of $\varepsilon''$ during aging, $\beta_{ag}$ is the stretched exponent ($\beta_{ag}(T < T_g) = \beta_{KWW}(T_g)$), and $\tau_{ag}$ is the aging time constant. For the selected temperature, irrespective of the chosen frequency, they obtained the same $\tau_{ag}$ (the aging time constant). The deduced values of $\tau_{ag}$ turned out to be nearly the same as $\tau_\alpha$ calculated from the coupling model (CM) [8–10] predicted relation between $\tau_\alpha$ and $\tau_\beta$, given via the primitive relaxation time $\tau_0$ by the following equations

$$\tau_\alpha = [(t_c)^{-n}\tau_0]^{1/(1-n)}, \qquad \tau_\beta \approx \tau_0 \quad (2)$$

where $t_c$ is about 2 ps for molecular and polymeric glassformers and $(1 - n)$ is the fractional exponent of the Kohlrausch–Williams–Watts (KWW) stretched exponential correlation function of the $\alpha$-relaxation [11]

$$\phi(t) = \exp[-(t/\tau_\alpha)^{1-n}]. \quad (3)$$

From this, CR concluded that 'the behavior of the $\tau_{ag}$ is consistent with its identification with $\tau_\alpha$ in the glassy state', and hence they successfully determined $\tau_\alpha$ from $\tau_\beta$ in the glassy state of poly(vinylethylene). The coincidence between the data from aging experiment $\tau_{ag}$ and values of $\alpha$-relaxation times calculated from the coupling model justifies the 'use of aging induced changes in JG relaxation to follow the structural dynamics in the glassy state', and 'a correlation between $\alpha$ and JG relaxations persist even in the glassy state' [7].

In view of the success of the method proposed by Casalini and Roland, we applied it to Telmisartan (TEL), a drug commonly prescribed to patients with high blood pressure. TEL has a well-separated Johari–Goldstein (JG) type $\beta$-process. Thus, the coupling model relation (equations (2)) can be used to predict $\alpha$-relaxation times $\tau_\alpha^{CM}$ from $\tau_\beta$ in the glassy state.

## 2. Experimental details

### *2.1. Material*

Telmisartan was supplied from Dr Reddy's Laboratories Limited (India, CAS No. 14470-48-4, purity $\geqslant$ 98%) and received as a white crystalline powder. Telmisartan is properly described chemically as 4′-[(1,4′-dimethyl-2′-propyl[2,6′-bi-1H-benzimidazol]-1′-yl)methyl]-[1,1′-biphenyl]-2-carboxylic acid. Its empirical formula is $C_{33}H_{30}N_4O_2$, its molecular weight is 514.63 g mol$^{-1}$, and its chemical structure is presented in figure 1. The obtained material was used without further purification.

### *2.2. Method—broadband dielectric spectroscopy (BDS)*

For the dielectric aging experiment we used an analogous setup and sample cell as described in [12]. The method of preparation amorphous TEL was also exactly the same. The sample was aged at a few different temperatures for up to five days. The temperature was kept stable to better than 0.1 K.

## 3. Results and discussion

In figure 1 we present dielectric loss spectra of TEL, measured at atmospheric pressure above (panel (a)) and below (panel (b)) the glass temperature. The glass transition temperature $T_g$ was defined as the temperature at which the dielectric relaxation time $\tau_\alpha$ is equal to 100 s. By extrapolating the Vogel–Fulcher–Tammann fit to $\tau_\alpha$ obtained from the loss peak frequencies for $T \geqslant 405.15$ K down to lower temperatures, the value of $T_g$ is 400.3 K [12]. For the sake of clarity, the dc-conductivity has been subtracted from the measured dielectric loss in the spectra shown above $T_g$. The dielectric $\alpha$-loss peak can only be seen in the dielectric spectra collected at temperatures 5 K or more above $T_g$. The secondary $\beta$-relaxation is barely visible in the $\varepsilon''(f)$ spectra at temperatures just above $T_g$ because its amplitude is small. Below $T_g$, it appears as a well defined $\beta$-peak albeit extremely broad. At the lowest temperatures, another faster secondary process (designated as $\gamma$) appears. Unfortunately it cannot be characterized because it did not show up completely within the experimental window[3].

We superpose the $\alpha$-loss peak part of $\varepsilon''(f)$ obtained at temperatures from 409.15 up to 459.15 K at ambient pressure by shifting the data at the higher temperatures to superpose them together with the unshifted data at 409.15 K. The good superposition of the $\alpha$-loss peak part indicates that the shape of the structural peak is practically invariant with temperature change (see figure 2 inset). In other words, time–temperature superposition holds in this temperature range. If we assume that the frequency dispersion of the $\alpha$-loss peak continues to be the same at all temperatures below 409.15 K, where the peak frequency is at about $2 \times 10^{-1}$ Hz, down to 373.15 K, deep in the glassy state, then we can approximately construct the $\varepsilon''(f)$ at 373.15 K by shifting the measured data of $\varepsilon''(f)$ at higher temperatures horizontally to superimpose them. This was carried out with the $\varepsilon''(f)$ data at four temperatures higher than 373.15 K, including 409.15 K, and the constructed and supposedly complete $\varepsilon''(f)$ data at 373.15 K is shown in the main part of figure 2. The black solid line represents the imaginary part of the one-sided Fourier transform of the time derivative of the KWW function in equations (2) with $(1 - n) \equiv 0.61$. This is actually the same KWW function that fits the $\alpha$-loss peak at 409.15 K because of the manner in which the loss peak at 373.15 K was artificially constructed. The solid green line represents the fit by the Havriliak–Negami (HN) function. The main panel of figure 2 clearly shows that the KWW function cannot describe the data at higher

[3] Since in this paper we would like to concentrate on the prediction of the structural relaxation times in the glassy state of TEL, here we are giving only the more important facts about the molecular dynamics of TEL. For detailed analysis of the molecular dynamics of the drug we would like to referred readers to our previous publication [12].

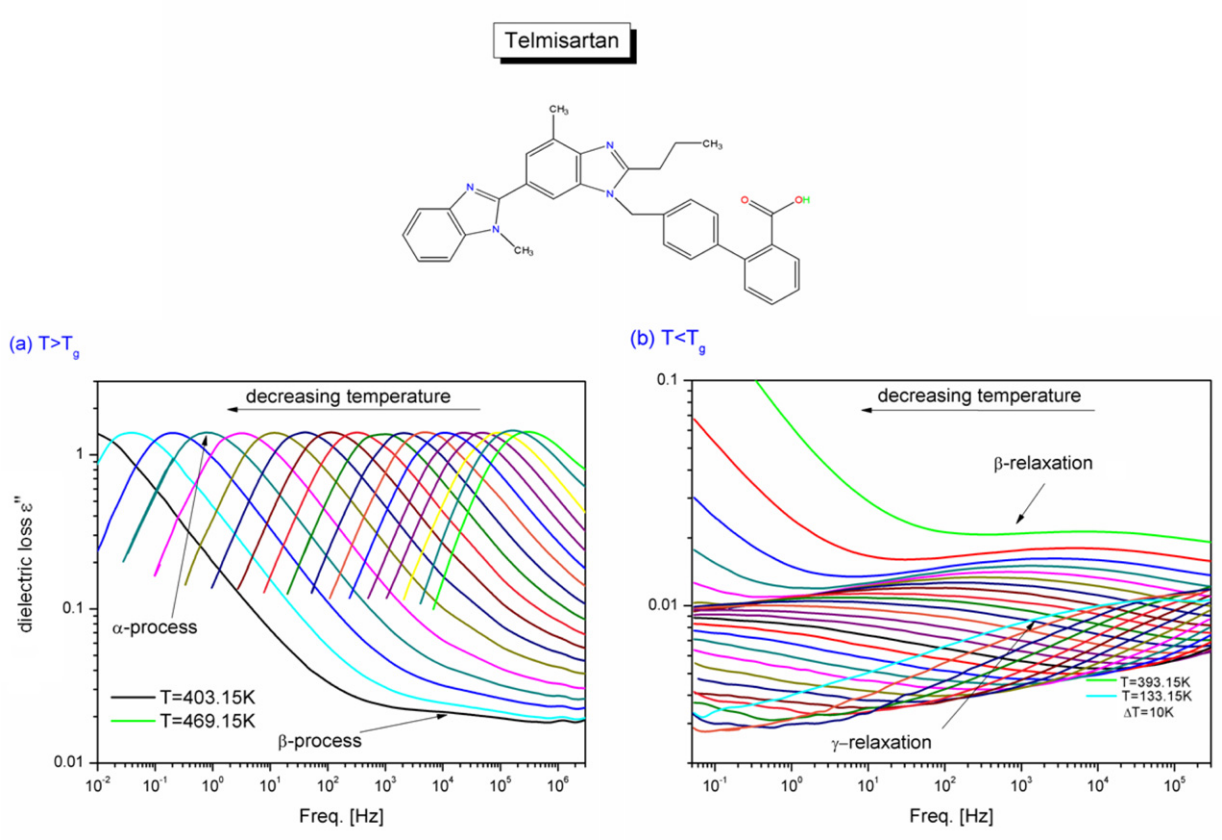


**Figure 1.** Dielectric loss spectra of TEL obtained on cooling at ambient pressure ($p = 0.1$ MPa) [11]. The panel (a) presents dielectric loss above the glass transition temperature between temperatures 469.15 and 403.15 K, after subtracting the conductivity, whereas panel (b) is in the glassy state. Above both panels we present the chemical structure of TEL.

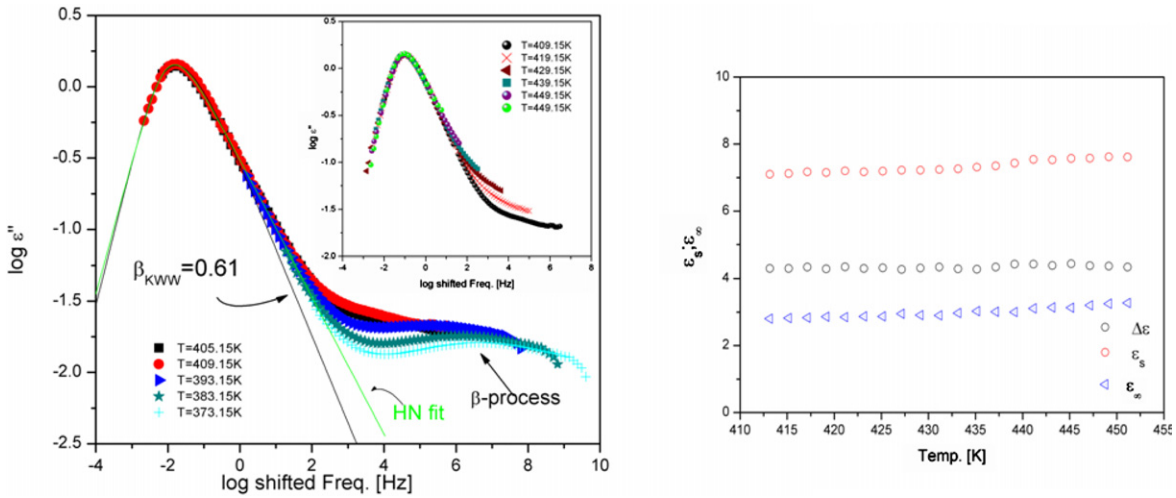


**Figure 2.** Left panel [11]—in the inset, we superpose the $\alpha$-loss peak part of $\varepsilon''(f)$ obtained at temperatures from 409.15 up to 459.15 K at ambient pressure by shifting the data at higher temperatures to superpose them all together with the unshifted data at 409.15 K. A good superposition of the $\alpha$-loss peak part is obtained. In the main figure, assuming the shape of the frequency dispersion of the $\alpha$-loss peak part of $\varepsilon''(f)$ is the same at 373.15 K, deep in the glassy state, as at 409.15 K, where the peak frequency is at about $2 \times 10^{-1}$ Hz, the $\varepsilon''(f)$ data at four temperatures higher than 373.15 K, including 409.15 K, are shifted horizontally to form a master $\alpha$-loss peak. The black solid line represents the KWW fit with $(1 - n) \equiv \beta_{\mathrm{KWW}} = 0.61$. The solid green line represents the Havriliak–Negami fit. Right panel—static permittivity, high frequency permittivity and dielectric strength, $(\Delta\varepsilon = \varepsilon_s - \varepsilon_\infty)$ as a function of temperature in the supercooled state of TEL.

frequencies as well as the HN function. However, the less satisfactory fit by the KWW function looms large only in the plot of $\log \varepsilon''(f)$ versus $\log f$, and the deviation at higher frequencies shows up as an apparent excess wing. However, in a semi-log plot of $\varepsilon''(f)$ against $\log f$, the discrepancies at high frequencies are actually small and could be contributed by

a faster process in the evolution of dynamics from the local $\beta$-relaxation to the cooperative $\alpha$-relaxation. Although a better fit to the structural relaxation peak at higher frequencies is obtained by the empirical HN function, it does not necessarily have a fundamental physical meaning superior to that of the KWW fit. In the supercooled liquid state of TEL the exponents $\alpha_{\mathrm{HN}}$ and $\beta_{\mathrm{HN}}$ of the HN fits have nearly constant values of $\alpha_{\mathrm{HN}} \approx 0.92$ and $\beta_{\mathrm{HN}} \approx 0.5$.

From the resolved $\beta$-loss peaks in the glassy state and at temperatures slightly above $T_{\mathrm{g}}$, their peak frequencies $f_\beta$ and the corresponding relaxation times $\tau_\beta$ have been determined. The Arrhenius temperature dependence of $\tau_\beta$ in the glassy state has been determined by $1/(2\pi f_{\max})$. Its activation energy $E_\beta$ has the considerably large value of 81.8 kJ mol$^{-1}$, which suggests that the $\beta$-relaxation involves the motion of the entire TEL molecule, and satisfies one of the several criteria for identifying the $\beta$-relaxation as the universal Johari–Goldstein (JG) $\beta$-relaxation of TEL [13]. Figure 3 shows the presence of the $\beta$-relaxation as a broad shoulder in the $\varepsilon''(f)$ spectrum at 405.15 K. The primitive frequency $f_0 \equiv (1/2\pi\tau_0)$, calculated by equations (2), serving as an estimate of $f_\beta$ is located within the broad shoulder, and hence this supports the observed $\beta$-relaxation of TEL being the JG process. The black dotted line shown in figure 3 is a fit to the shoulder by a symmetrical Cole–Cole function. The peak frequency of the Cole–Cole function is slightly less than 1 decade higher than $f_0$, but the width of the Cole–Cole fit is so broad that it is meaningless to stress the difference. Besides, the various correlations and connections exhibited by the JG relaxation to the $\alpha$-relaxation found experimentally [13–17] rule out the JG process being represented in the loss spectrum as an additive contribution to the $\alpha$-relaxation suggested by the Cole–Cole fit. Furthermore, the equation involving $E_\beta$ and the prefactor $\tau_\infty$ in the Arrhenius dependence of $\tau_\beta$ given by [18]

$$E_\beta/RT_{\mathrm{g}} = 2.303(2 - 13.7n - \log\tau_\infty) \qquad (4)$$

can be used as another test if the $\beta$-process is the JG secondary relaxation. The left side of the above equation is equal to 24.57, whereas the right side gives 28.89. Taking into consideration the large uncertainties involved in the determination of $\tau_\beta$, the comparable values obtained from the left and right sides serve as further evidence that the $\beta$-process is the JG relaxation of TEL. Moreover, the ratio $E_\beta/RT_{\mathrm{g}} = 24.57$ for TEL is in good agreement with the value of 24 found by Kudlik *et al* [19] for the secondary relaxation in several glassformers.

### *3.1. Aging experiment*

The TEL sample was aged and the change of the $\beta$-loss peak was observed at several chosen temperatures: 393.15, 373.15, 353.15 and 333.15 K. For the sake of clarity, in this paper we will present the results of the aging experiment only for one arbitrarily chosen temperature. Figure 4(a) shows the $\varepsilon''(f)$ dependence at 373.15 K for different aging times. Under this condition, only the $\beta$-peak is observed within the experimental frequency window. With an increase in aging time $t_{\mathrm{ag}}$, the glass is further densified and, consequently, the amplitude of local motion and hence the intensity of the $\beta$-loss is reduced.

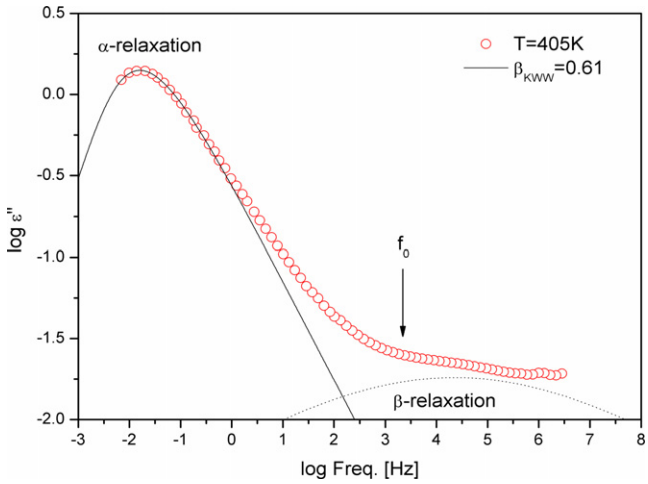


**Figure 3.** Dielectric loss of TEL versus frequency at 405 K under atmospheric pressure. The arrow indicates the location of the calculated frequency $f_0$ of the primitive process.

The peak frequency of the $\beta$-loss however remains practically unchanged. Consequently, the separation of the $\alpha$-relaxation from the $\beta$-relaxation increases on aging, and in the context of equations (2) of the coupling model this means that the coupling parameter $n \equiv (1 - \beta_{\mathrm{KWW}})$ must increase on aging. We shall return to this point later.

Similar changes were obtained for other temperatures, although at lower temperature the system needs more time to approach the equilibrium value of $\varepsilon''$. For three fixed frequencies we plot $\varepsilon''(\tilde{f}, t_{\mathrm{ag}})$ dependences normalized by the factor $\varepsilon''(\tilde{f}, t_{\mathrm{ag}} = 0)$, as shown in figure 4(b). To describe the $\varepsilon''(\tilde{f}, t_{\mathrm{ag}})$ dependences we used the stretched exponential function proposed by Casalini and Roland. The best fits of equation (1) are displayed as black solid lines. To fit the data we used a fixed value of the stretching parameter $\beta_{\mathrm{ag}} = 0.61$, as determined from the fitting of the structural relaxation peak above $T_{\mathrm{g}}$. Similar to what was done for PVE, we have assumed that the shape of the $\alpha$-peak does not change below the glass transition temperature ($\beta_{\mathrm{ag}}(T < T_{\mathrm{g}}) = \beta_{\mathrm{KWW}}(T_{\mathrm{g}}) = 0.61$). It is worth pointing out that the fitting function with fixed $\beta_{\mathrm{ag}} = 0.61$ does not describe the experimental data precisely (see figure 4(b)).

For the three sets of data presented in figure 4(b) (at different frequencies) we get almost the same $\tau_{\mathrm{ag}}$, which suggests that the results from these analyses are frequency independent. To ensure that $\tau_{\mathrm{ag}}$ does not change considerably during the aging experiment, the data were divided into few intervals (covering, overlapping and exceeding the whole time range of the experiment) and simultaneously fitted to equation (1). We allowed $\tau_{\mathrm{ag}}$ to vary independently. As it turned out, the value of $\tau_{\mathrm{ag}}$ for different intervals does not change that much (within experimental error). The same analyses were also made for the other three temperatures. The $\tau_{\mathrm{ag}}(1/T)$ dependence is shown in the relaxation map of TEL (figure 5—red stars).

In addition, to get information about the structural relaxation times below $T_{\mathrm{g}}$, we also adopt a more simple method i.e. a selected $\alpha$-peak, located just above $T_{\mathrm{g}}$

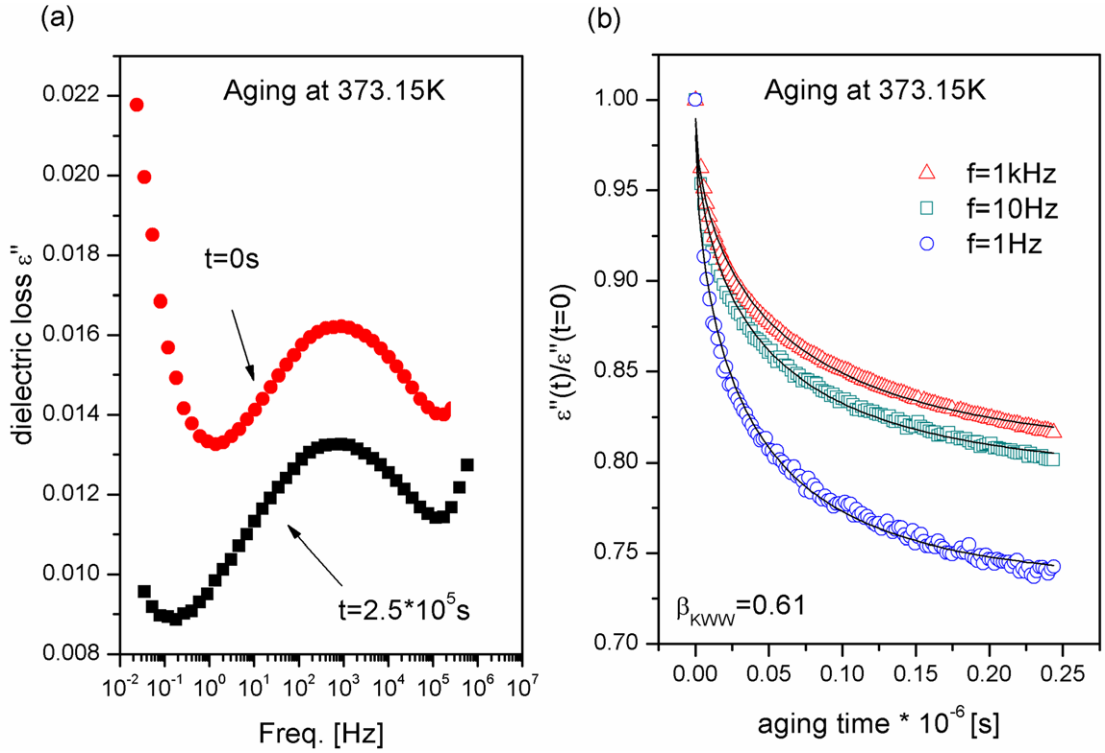


**Figure 4.** Left panel (a) dielectric loss spectra at $T = 373.15$ K during physical aging; right panel (b) dielectric loss (normalized by the loss at $t_{ag} = 0$ s) versus aging time for three fixed frequencies. Normalized $\varepsilon''$ decreases were fitted to the equation (1). All curves can be described by the same time constant $\tau_{ag}$, irrespective of the chosen frequency [11].

($T = 407.15$ K), was shifted horizontally to the temperatures below $T_g$ so that its high frequency side superimposes with the low frequency side of spectra collected below $T_g$. Obviously, this operation required the assumption that the shape of the structural relaxation peak does not change much below $T_g$ and the time–temperature superposition (TTS) is valid above and below $T_g$. The values of relaxation times $\tau_{\alpha-sup}$, obtained in this way, plotted versus $1/T$ are shown in figure 5 (gray triangles). Nevertheless, it is worth mentioning that this procedure gives reliable values of structural relaxation times (for $T < T_g$), but only in the vicinity of the glass transition, where the evolution of the glassy system towards equilibrium is quite fast. This situation is very different at lower temperatures where the system evaluates slower. Thus, the relaxation times $\tau_{\alpha-sup}$ obtained, as well as $\beta_{KWW} = 0.61$ assumed deep in the glassy state, are subject to uncertainty.

Finally, the values of $\tau_{ag}$, $\tau_{\alpha-sup}$ and $T_0 = 317.81$ K [12] all indicate that the timescale of molecular motion involved with the $\alpha$-relaxation at room temperature probably exceeds years.

### *3.2. α-relaxation times in the glassy state calculated by the coupling model*

Using the coupling model (CM) approach (equations (2) and (3)) we can calculate $\tau_\alpha^{CM}$ of TEL in the glassy state from the known values of $\tau_\beta$. The calculation requires the coupling parameter $n$ or its complement $(1 - n) \equiv \beta_{KWW}$ in the glassy state, which cannot be directly determined because $\tau_\alpha$ is too long. One choice is to use the same value of $\beta_{KWW} = 0.61$ determined by fitting the isothermal loss spectra at $T \geqslant 409.15$ K. In doing so, the assumption is made that the frequency dispersion of the $\alpha$-relaxation does not change for $T < T_g = 400.3$ K. The results presented in the relaxation map of TEL (figure 5, open green up triangles) show $\tau_\alpha^{CM}$ substantially underestimates $\tau_{ag}$. However, before taking this glaring disagreement seriously, one must reconsider the fact that CM only predicts approximate agreement between the primitive relaxation time $\tau_0$ and a characteristic relaxation time of the $\beta$-relaxation $\tau_\beta$. In other glassformers which have a well resolved JG $\beta$-loss peak above $T_g$, the width of the $\beta$-loss peak is usually not very broad. In these cases, $\tau_\beta$ can be taken to be $1/2\pi f_p$, where $f_p$ is the frequency of peak maximum. However, the situation is different for TEL. Even above $T_g$, the $\beta$-relaxation appears as a very broad shoulder (see figure 1(a)). Below $T_g$, the width of the $\beta$-loss peak is even larger. The values of $\tau_0$ used to calculate $\tau_\alpha^{CM}$ were taken to be $\tau_\beta$, plotted in figure 5, and $\tau_\beta \equiv 1/2\pi f_p$, where $f_p$ is the frequency of the peak maximum. If $\hat{f}_p$ is taken to be 1.7 decades lower than $f_p$, one can estimate from the flat loss $\beta$-loss peaks in figure 1(b) that $\varepsilon''(\hat{f}_p)$ is only about 10% less than $\varepsilon''(f_p)$. Thus, this choice of $\hat{f}_p$ is as valid as $f_p$ to stand for the characteristic $\beta$-relaxation frequency $f_\beta$, and $\hat{\tau}_\beta \equiv 1/(2\pi \hat{f}_p)$ for the corresponding characteristic $\beta$-relaxation time. If we take $\tau_0 = \hat{\tau}_\beta$ (figure 5, black closed squares), together with the assumed $\beta_{KWW} = 0.61$, to calculate $\hat{\tau}_\alpha^{CM}$ by equations (2), there is now good agreement between

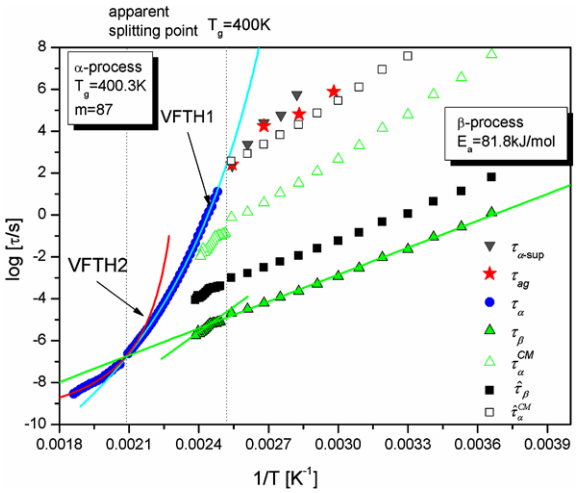


**Figure 5.** Relaxation map of TEL. The temperature dependence of $\tau_\alpha$ above $T_g$ was described by two VFTH equations. The relaxation times of the $\alpha$-process in the glassy state were estimated in two different ways: by a horizontal shift of the $\alpha$-peak from the region above $T_g$ to temperatures below $T_g(\tau_{\alpha-\mathrm{sup}})$, and by using aging induced changes in the JG relaxation in accordance with [7] ($\tau_{\mathrm{ag}}$). The structural relaxation times $\tau_\alpha^{\mathrm{CM}}$ shown by open green up triangles are calculated using CM with $\beta_{\mathrm{KWW}} = 0.61$, and $\tau_\beta \equiv 1/(2\pi f_\mathrm{p})$ represented by closed green up triangles, where $f_\mathrm{p}$ is the peak frequency of the $\beta$-loss peak in figure 1(b). The temperature dependence of $\tau_\beta(T)$ is Arrhenius below $T_g$ but changes to a stronger $T$-dependence above $T_g$. The structural relaxation times $\hat{\tau}_\alpha^{\mathrm{CM}}$ shown by open black squares are calculated using CM with $\beta_{\mathrm{KWW}} = 0.61$, and $\hat{\tau}_\beta \equiv 1/(2\pi \hat{f}_\mathrm{p})$ represented by closed black squares, where $\hat{f}_\mathrm{p}$ is 1.7 decades lower than $f_\mathrm{p}$.

$\hat{\tau}_\alpha^{\mathrm{CM}}$ and $\tau_{\mathrm{ag}}$ (see figure 5, open black squares). On the other hand, had we used $\hat{f}_\mathrm{p}$, which is 1.7 decades not lower but higher than the $f_\mathrm{p}$, to calculate $\hat{\tau}_\beta$, the value of structural relaxation time obtained from the CM formula $\tau_\alpha^{\mathrm{CM}}$ would become so short that it is absurd for a structural relaxation time in the glassy state. If one insists that $\tau_0$ be taken the same as $\tau_\beta \equiv 1/2\pi f_\mathrm{p}$, then there is serious inconsistency between the values of the calculated $\tau_\alpha^{\mathrm{CM}}$ and the observed aging time $\tau_{\mathrm{ag}}$. However, one also has to bear in mind the large uncertainty in identifying the characteristic $\beta$-relaxation time for TEL from the very broad maximum of the $\beta$-peak, the fact that the CM only predicts an order of magnitude agreement between $\tau_0$ and the characteristic $\beta$-relaxation time, and the possible increase of the coupling parameter $n$ upon aging instead of the assumed constant value from $\beta_{\mathrm{KWW}} = 0.61$ used for the comparison. The last point is cogent in the present case, since $\tau_{\mathrm{ag}}$ shifts to longer times on aging but $\tau_\beta$ does not, and this requires an increase of $n$ in order to be consistent with the CM equation.

### *3.3. The change of representation from susceptibility to electric modulus*

As shown in the previous section, due to the very broad flat maximum of the $\beta$-loss peak, the identification of a characteristic $\beta$-relaxation time with the primitive relaxation time poses a problem. So far, all isothermal and aging data have been presented as a complex susceptibility $\varepsilon^*(f)$, which is of course a standard and appropriate representation. However, in this section we explore the same data and analysis in terms of the complex electric modulus, $M^*(f) \equiv 1/\varepsilon^*(f)$. It enable us to demonstrate another point of view on the overall situation associated with determination of structural relaxation times in TEL and stress some essential differences between presentation of same dielectric data in various representations, especially in the case of materials with large dielectric strength, as in the present case of TEL.

Dielectric susceptibility and electric modulus formalisms reflect two alternative ways for the description of dielectric phenomena. In the first one, time-dependent variation of dielectric displacement vector **D**, under constant electric field **E**, is recorded [20], while for the second one the constraint of a constant dielectric displacement **D** is applied and variation of the electric field **E** with time is recorded [20]. It is worthwhile stressing that $\varepsilon^*(\omega)$ as well as $M^*(\omega)$ reflect the same dynamics of orientational polarization of permanent dipoles [21], albeit under different **E** and **D** conditions.

The electric modulus representation is practically used only for describing ion dynamics, particularly in ionic conductors [22, 23]. A review of the electric modulus representation, and answers to criticism of its usage can be found in [24]. Before using the electric modulus formalism here, let us re-examine the dielectric permittivity function, which is often called the 'dielectric relaxation function'. It actually describes, not dielectric relaxation, but retardation of the buildup of the condenser charge after a step potential is applied, while the electric modulus function directly refers to the dielectric relaxation of the condenser potential after the application of a step charge [25–28]. It is also worth noting that relaxation is in general faster than retardation, i.e. the decay of the electric modulus response function $\phi_M(t)$ takes less time than the time-dependent permittivity response function $\phi_\varepsilon(t)$ [25, 26]. As a result, for a simple Debye-type relaxation at fixed temperature the characteristic relaxation time $\tau_M$ is faster than the retardation time $\tau_\varepsilon$, in accordance with following equation

$$\tau_M \left( \frac{\varepsilon_s}{\varepsilon_\infty} \right) = \tau_\varepsilon \tag{5}$$

where $\varepsilon_s$ and $\varepsilon_\infty$ are dielectric constants in the limits of low and high frequency, respectively. In particular, for a non-Debye distribution of relaxation times the difference between $\tau_M$ and $\tau_\varepsilon$ become even more pronounced, and the effect on the dispersion of the relaxation–retardation timescale ratio should also be taken into account [27].

To demonstrate how the ratio of dielectric constants $\frac{\varepsilon_\infty}{\varepsilon_s}$ influences the shape and characteristic relaxation time during switching from one representation to another, we present some simultaneously generated relaxation peaks with different dielectric strength. For example, for a polar liquid with dielectric strength equal to 7 ($\varepsilon_s = 8, \varepsilon_\infty = 1$) and 4 ($\varepsilon_s = 5, \varepsilon_\infty = 1$), the Cole–Davidson-type relaxation function

$$\varepsilon^*(\omega) = \varepsilon_\infty + \frac{\varepsilon_s - \varepsilon_\infty}{[1 + (\mathrm{i}\omega\tau_\varepsilon)^\alpha]^\beta}, \qquad \alpha = 1, \quad \beta = 0.5 \tag{6}$$

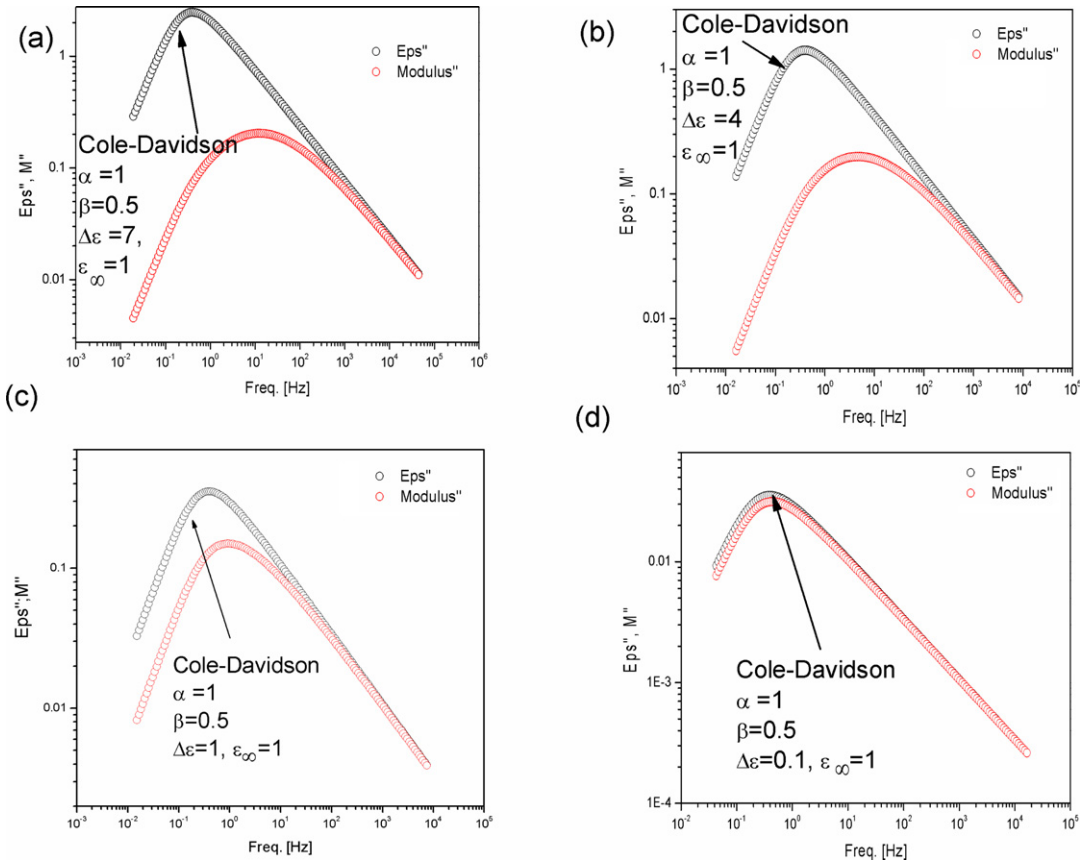


**Figure 6.** Plots of the imaginary part of dielectric permittivity/modulus versus frequency for a CD-type dielectric function, generated for various different dielectric strength $\Delta\varepsilon = 7$ (a), $\Delta\varepsilon = 4$ (b), $\Delta\varepsilon = 1$ (c) and $\Delta\varepsilon = 0.1$ (d). The $\varepsilon''(\omega)$ curves were transformed to electric modulus $M''(\omega)$. The greater the dielectric strength, the more the relaxation peak in $M''(\omega)$ shifts to a faster response, becoming broader and smaller compared to the CD case.

generated in the susceptibility representation and later transformed to the electric modulus representation, becomes much smaller but broader, and its relaxation time $\tau_M$ is shifted more than 1 decade (for $\Delta\varepsilon = 4$) and 2 decades (for $\Delta\varepsilon = 7$) towards a faster response relative to the CD case (see figures 6(a) and (b)). However, for a system with very low dielectric strength, these differences become considerably smaller or even negligible (figures 6(c) and (d)).

From this simple exercise it is clearly seen that for materials with small dielectric strength the two choices of representation (susceptibility or electric modulus) do not bring significant changes in the shape and position of the dipolar relaxation peak. However, for highly polar systems we may expect substantial differences between the shape and the position of the relaxation peak in the two representations. Furthermore, it is worth mentioning that the change of representation does not change the power-law behavior on the sides of the loss peaks.

We have transformed the $\varepsilon^*(f)$ data of TEL to $M^*(f)$, which is simply the reciprocal of $\varepsilon^*(f)$, i.e.

$$M^*(f) = 1/\varepsilon^*(f). \tag{7}$$

Similar to the effects seen in the simulation, the $\alpha$-loss peak in the $M''(f)$ spectra is shifted to higher frequencies and becomes smaller and broader. This is demonstrated in figure 7 when compared with the data of $\varepsilon''(f)$ at the same temperatures presented in figure 1. Similarly, in the $M''(f)$ spectra, the structural relaxation peak moves towards lower frequencies with decreasing temperature. In the modulus representation,

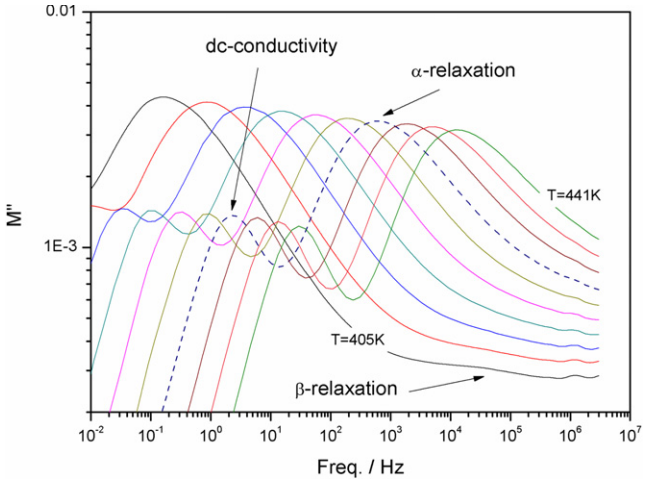


**Figure 7.** Frequency dependence of the imaginary part of the electric modulus of TEL for various temperatures above $T_g$.

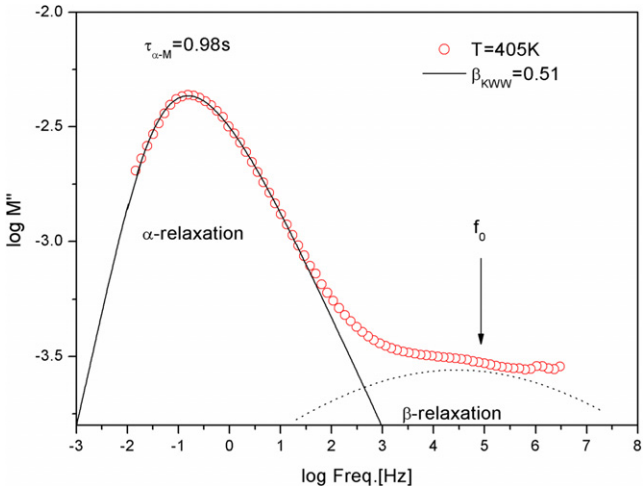


**Figure 8.** Frequency dependence of the imaginary part of the electric modulus at 405 K under atmospheric pressure. The arrow indicates the location of the calculated frequency $f_0$ of the primitive process.

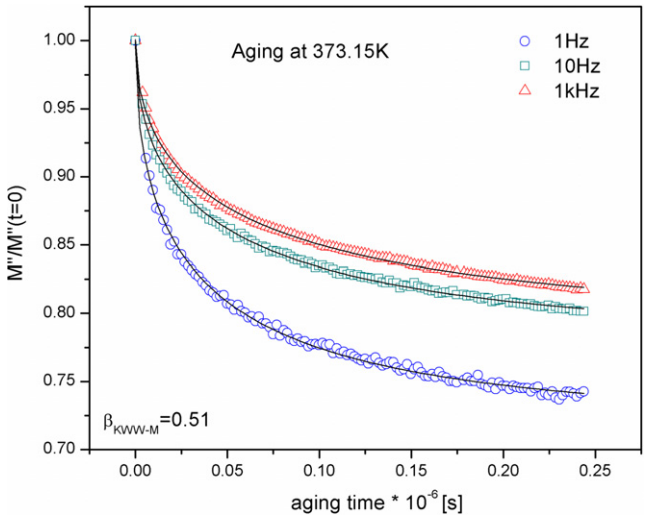


**Figure 9.** The normalized imaginary part of the electric modulus versus aging time for three different frequencies. The decrease of $M''$ was fitted to equation (8) with fixed $\beta_{\mathrm{KWW}-M} = 0.51$ (solid black lines). All three curves can be described with the same time constant $\tau_{\mathrm{ag}}$, irrespective of the chosen frequency.

the translational motion of ions appear as the Debye peak, whereas the $\alpha$-peak is shifted about 2 decades to higher frequencies still corresponding to the orientational relaxation of molecules.

To describe the non-exponential character of molecular relaxation by the KWW function, a smaller stretching parameter ($\beta_{\mathrm{KWW}-M} = 0.51$) has to be used to fit the $M''$ $\alpha$-loss peak. It is noticeable that the power-law behavior described by the stretching parameter $\beta_{\mathrm{KWW}-M}$ agrees with that given by the HN function in the susceptibility representation ($\beta_{\mathrm{HN}} \approx 0.5$). Furthermore, it is worth pointing out that at the same temperature the KWW function fits the $\alpha$-loss peak at higher frequencies better in the modulus representation than in the susceptibility representation. Using equation (2) with $\tau_{\alpha-M} = 0.41$ s and $\beta_{\mathrm{KWW}-M} = 0.51$, the location of the calculated primitive frequency $f_0$ in the modulus formalism is indicated by the vertical arrow in figure 8. This is to be compared with its location in the susceptibility representation and its relation to the shoulder contributed by the $\beta$-process shown in figure 3. At the same temperature (405 K), the same data presented in the modulus formalism has the primitive frequency clearly lying within the $\beta$-peak, which makes it easier to identify the nature of the $\beta$-relaxation.

### *3.4. Analyzing data of the aging experiment in the modulus representation*

Returning to the data obtained in the aging experiment, we make an attempt to analyze them in terms of the imaginary part of electric modulus $M''(\tilde{f}, t_{\mathrm{ag}})$ of TEL and its change with aging time $t_{\mathrm{ag}}$. For three fixed frequencies we plot $M''(\tilde{f}, t_{\mathrm{ag}})$ dependences normalized by the factor $M''(\tilde{f}, t_{\mathrm{ag}} = 0)$ as shown in figure 9. Similarly, to fit the aging data we used equation (1), but modified it for the modulus data. It has the form,

$$\frac{M''(\tilde{f}, t_{\mathrm{ag}})}{M''(\tilde{f}, t_{\mathrm{ag}=0})} = \left\{ \Delta M''(\tilde{f}, t_{\mathrm{ag}}) \times \exp\left[ -\frac{t_{\mathrm{ag}}}{\tau_{\mathrm{ag}}} \right]^{\beta_{\mathrm{ag}}} + M''_{\mathrm{eq}}(\tilde{f}) \right\} \Big/ M''(\tilde{f}, t_{\mathrm{ag}=0}), \tag{8}$$

where $M''_{\mathrm{eq}}(\tilde{f}) \equiv M''(\tilde{f}, t_{\mathrm{ag}} \to \infty)$ is an equilibrium value, $\Delta M''(\tilde{f}, t_{\mathrm{ag}}) = M''(\tilde{f}, t_{\mathrm{ag}} = 0) - M''_{\mathrm{eq}}$ is the change of $M''$ during aging, $\beta_{\mathrm{ag}}$ is the stretched exponent ($\beta_{\mathrm{ag}}(T < T_{\mathrm{g}}) = \beta_{\mathrm{KWW}-M}(T > T_{\mathrm{g}})$), and $\tau_{\mathrm{ag}}$ is the aging time constant. The best fits of equation (8) are displayed in figure 9 as solid black lines. It can be seen from figure 9 that fitting functions with the fixed value of $\beta_{\mathrm{KWW}-M} = 0.51$ give better fits than for the same data in the susceptibility representation with $\beta_{\mathrm{KWW}} = 0.61$ (see figure 4). Here again, irrespective of the chosen frequency, we get almost the same $\tau_{\mathrm{ag}}$. The same analyses were also made for three other temperatures. The values of $\tau_{\mathrm{ag}}(1/T)$ are shown in the relaxation map of TEL constructed for the modulus data (figure 10—red triangles). The corresponding $\tau_{\mathrm{ag}}$ are only slightly different from those obtained for $\varepsilon''(\tilde{f}, t_{\mathrm{ag}})$ dependences. All other relaxation times are also from the analyses of data in the modulus representation.

When considering aging experiments investigating the imaginary parts of the dielectric permittivity $\varepsilon''$ and dielectric modulus $M''$, it is worth recalling measurements performed a few years ago by Lunkenheimer *et al* [29–31], in which several glass-forming liquids, such as PC, CKN, xylitol or glycerol, were aged. Their studies were limited only to the temperature region just below $T_{\mathrm{g}}$, where in addition the $\beta$-relaxation was partly/completely covered by the $\alpha$-relaxation. This is completely unlike our case, since the aging we carried out was in a region where the $\beta$-relaxation was well-separated from the structural relaxation time. What is worth noting is that Lunkenheimer and co-workers make an effort to analyze the

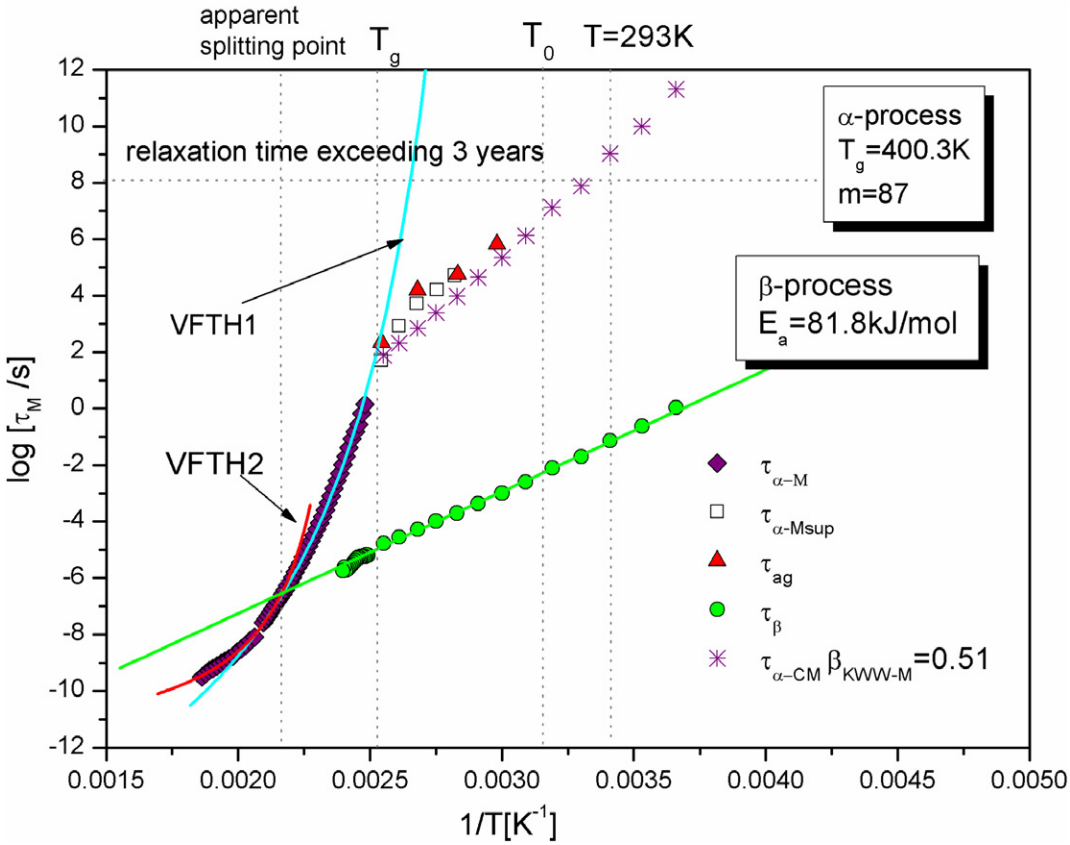


**Figure 10.** Temperature dependence of $\alpha$- and $\beta$-relaxation times of TEL obtained from frequency dependences of the imaginary part of the electric modulus, along with the aging decay time $\tau_{ag}$, $\tau_{\alpha-M\,sup}$ and $\tau^{CM}_{\alpha-M}$ calculated from the CM (with $\beta_{KWW-M} = 0.51$) in the glassy state.

aging data of ionically conducting CKN in the susceptibility as well as modulus representation. In the $M''$ spectra, due to a large decoupling effect, the peak was aged, while in the $\varepsilon''$ spectra the dc-conductivity was strongly influenced. Their studies revealed that the aging dynamics, irrespective of the chosen representation, show the same time dependence during aging, governed by the structural relaxation time and the same heterogeneity as in equilibrium [31].

It is obvious that the structure of glass depends on the aging time. However, in the temperature region close to $T_g$ the change of $\tau_{ag}$ with time is considerable higher than far below $T_g$, where it can be negligible. Because, in the vicinity of the glass transition, for the structure of glass evaluated towards equilibrium relatively fast, Lunkenheimer *et al* observed significant deviations (unlike in our case) between the values of $\tau_{ag}$ and the equilibrium data.

### *3.5. Calculation of the α-relaxation times in the glassy state by the coupling model*

Similar to before in using the prediction of the CM, we calculated $\tau_{\alpha-M}$ from $\tau_\beta$ in the glassy state. In the calculation we assumed that $\beta_{KWW-M}$ at temperatures below $T_g$ has the same value as at 405.15 K close to the $T_g$ i.e. $\beta_{KWW-M} = 0.51$. The results obtained are displayed in the relaxation map of TEL (figure 10—violet stars), where all the data are from the modulus representation. The values of $\tau_{\alpha-M}$ in the glassy state, calculated from the CM and shown in figure 10, are in a good agreement with $\tau_{ag}$ from the aging experiment.

Currently, the CM is commonly applied to describe successfully the dynamics of molecular supercooled liquids and also of ions in ionic conductors, using the susceptibility representation of data in the former case and the electric modulus representation in the latter case. This is possible because the CM is applicable independent of whether the correlation function is a relaxation function $\phi_{rel}$ or a retardation function $\phi_{ret}$. However, as shown in this paper, for very polar molecular glassformers such as TEL, $\phi_{rel}$ and $\phi_{ret}$ from the same data differ in the width of dispersion. Nevertheless, the primitive relaxation time/frequency calculated from the CM for both cases are consistent with that of the $\beta$-relaxation from experiment. Is it possible that the $\beta$-relaxation is also changed in going from the susceptibility representation to the modulus representation to maintain consistency with the CM predication? Further investigation is needed to understand whether this is not happenstance.

Finally, since crystallization from the amorphous state is often linked to the molecular mobility associated with structural relaxation, the results of this paper are important for the prediction of the stability of amorphous pharmaceuticals. It is commonly believed that stabilization of amorphous pharmaceuticals can be achieved by storage at a temperature where the molecular mobility associated with the instability of glass is negligible. At this temperature the structural relaxation

times would exceed years. For a pharmaceutical scientist, it seems to be necessary to have some useful tool allowing the probing of $\alpha$-relaxation times in the glassy state. This can be achieved by using the approach pioneered by CR, which in a very simply way provides reliable information about the timescale of structural relaxation below $T_g$. For TEL, the timescale of the $\alpha$-relaxation peak in the glassy state at room temperature most probably exceeds years. Thus, the molecular mobility associated with structural relaxation would be negligible in causing crystallization during typical storage at room temperature, and TEL should remain physically and chemically stable, over a prolonged period of time and a shelf-life of years.

## 4. Summary

To provide information about the timescale of structural relaxation deep in the glassy state of TEL, we applied a new approach suggested by Casalini and Roland. The analysis of aging induced changes in $\beta$-relaxation enables us to predict $\alpha$-relaxation times in the region inaccessible to standard dielectric techniques. There is an alternative method to determine the structural relaxation times in the glassy state of TEL. This method involves shifting horizontally the $\alpha$-loss peak observed near, but above $T_g$, to overlap the spectra collected below $T_g$. The structural relaxation time $\tau_{\alpha-\mathrm{sup}}$ in the glassy state, determined by this method, is in good agreement with that obtained by analyzing the aging data.

Furthermore, we calculate $\tau_\alpha$ from $\tau_\beta$ in the glassy state by using the CM relation (equations (2)). A large uncertainty cannot be avoided in picking where the characteristic relaxation time of the JG $\beta$-relaxation occurs because the $\beta$-loss peak in the $\varepsilon''(f)$ spectra is very broad. Within this uncertainty, there is consistency between the $\alpha$-relaxation time calculated by the CM equation and that deduced from the aging data.

We also made another attempt to analyze the aging susceptibility data in terms of the electric modulus representation. The results obtained for $\tau_{\mathrm{ag}}$ in the modulus representation are similar to those in the susceptibility representation, but the fitting function with the fixed value of $\beta_{\mathrm{KWW}-M} = 0.51$ gives a better fit than for the same data in the susceptibility representation with ($\beta_{\mathrm{KWW}} = 0.61$). In the electric modulus representation, the $\alpha$-relaxation calculated from the CM equation agrees with $\tau_{\alpha-\mathrm{sup}}$ and $\tau_{\mathrm{ag}}$ in the glassy state of TEL.

We also highlight that, for the same data presented in different types of representation, the shape and the peak position might differ significantly when considering materials with a large value of dielectric strength. In less polar glassformers, where the ratio $\varepsilon_s/\varepsilon_\infty$ is not large, the shape and position the of dipolar relaxation peak is not much different for the same data in either the susceptibility or the modulus representation. This is the case for PVE, which has $\Delta\varepsilon \approx 0.13$ [32]. However in polar glassformers with a large $\varepsilon_s/\varepsilon_\infty$, such as TEL, the shape and the position of the relaxation peaks are quite different. More study is needed to clarify the difference in spectral shape found in highly polar glassformers of the $\alpha$-relaxation, as well as the relationship between the $\alpha$- and the $\beta$-relaxation, in the susceptibility versus modulus representation.

## Acknowledgments

KA and MP are most grateful for financial support within the framework of the project entitled 'From Study of Molecular Dynamics in Amorphous Medicines at Ambient and Elevated Pressure to Novel Applications in Pharmacy', which is operated within the Foundation for Polish Science Team Programme co-financed by the EU European Regional Development Fund. KLN was supported by the Office of Naval Research.

## References

[1] Shmeis R A, Wang Z and Krill S K 2004 *Pharm. Res.* **21** 2031–9
[2] Shmeis R A, Wang Z and Krill S K 2004 *Pharm. Res.* **21** 2025–30
[3] Hancock B C, Shamblin S L and Zografi G 1995 *Pharm. Res.* **12** 799–806
[4] Shamblin S L, Tang X, Chang L, Hancock B C and Pikal M J 1999 *J. Phys. Chem.* B **103** 4113–21
[5] Vyazovkin S and Dranca I 2006 *Pharm. Res.* **23** 422–8
[6] Vyazovkin S and Dranca I 2005 *J. Phys. Chem.* B **109** 18637–44
[7] Casalini R and Roland C M 2009 *Phys. Rev. Lett.* **102** 035701
[8] Ngai K L and Rendell R W 1997 *Supercooled Liquids, Advances and Novel Applications* (*ACS Symposium Series* vol 676) ed J T Fourkas, D Kivelson, U Mohanty and K Nelson (Washington, DC: American Chemical Society) chapter 4, pp 45–66
[9] Ngai K L, Casalini R, Capaccioli S, Paluch M and Roland C M 2006 Dispersion of the structural relaxation and the vitrification of liquids *Fractals, Diffusion and Relaxation in Disordered Complex Systems* (*Advances in Chemical Physics* vol 133) ed Y P Kalmykov, W T Coffey and S A Rice (New York: Wiley) pp 79–138, ISBN: 0-471-72507-2
[10] Ngai K L 2003 *J. Phys.: Condens. Matter* **15** S1107
[11] Kohlrausch R 1847 *Ann. Phys., Lpz.* **72** 393
Williams G and Watts D C 1970 *Trans. Faraday Soc.* **66** 80–5
[12] Adrjanowicz K, Wojnarowska Z, Wlodarczyk P, Kaminski K, Paluch M and Mazgalski J 2009 *Eur. J. Pharm. Sci.* **38** 395–404
[13] Ngai K L and Paluch M 2004 *J. Chem. Phys.* **120** 857
[14] Mierzwa M, Pawlus S, Paluch M, Kaminska E and Ngai K L 2008 *J. Chem. Phys.* **128** 044512
[15] Kessairi K, Capaccioli S, Prevosto D, Lucchesi M, Sharifi S and Rolla P A 2008 *J. Phys. Chem.* B **112** 4470
[16] Böhmer R, Diezemann G, Geil B, Hinze G, Nowaczyk A and Winterlich M 2006 *Phys. Rev. Lett.* **97** 135701
[17] Nowaczyk A, Geil B, Hinze G and Böhmer R 2006 *Phys. Rev.* E **74** 041505
[18] Ngai K L and Capaccioli S 2004 *Phys. Rev.* E **69** 031501
[19] Kudlik A, Tschirwitz C, Benkhof S, Blochowicz T and Rössler E 1997 *Europhys. Lett.* **40** 649
[20] Fröhlich H 1958 *Theory of Dielectrics* (Oxford: Clarendon)
[21] Richert R and Wagner H 1997 Dielectric relaxation under constant charge conditions *Recent Research Developments in Macromolecules Research* vol 2, ed S G Pandalai (Trivandrum: Research Signpost) pp 1–10
[22] Macedo P B, Moynihan C T and Bose R 1972 *Phys. Chem. Glasses* **13** 171–9
Roling B, Happe A, Funke K and Ingram M D 1997 *Phys. Rev. Lett.* **78** 2160–3

[23] Howell F S, Bose R A, Macedo P B and Moynihan C T 1974 *J. Phys. Chem.* **78** 639
[24] Hodge I M, Ngai K L and Moynihan C T 2005 *J. Non-Cryst. Solids* **351** 104–15
[25] Wagner H and Richert R 1997 *Polymer* **38** 255–61
[26] Jäckle J and Richert R 2008 *Phys. Rev.* E **77** 031201
[27] Ito N and Richert R 2005 *J. Chem. Phys.* **123** 106101
[28] Richert R and Wagner H 1998 *Solid State Ion.* **105** 167–73
[29] Lunkenheimer P, When R, Schneider U and Loidl A 2005 *Phys. Rev. Lett.* **98** 055702
[30] Lunkenheimer P, When R and Loidl A 2006 *J. Non-Cryst. Solids* **353** 4941–5
[31] When R, Lunkenheimer P and Loidl A 2007 *J. Non-Cryst. Solids* **353** 3862–70
[32] Smith G D and Bedrov D 2006 *Eur. Polym. J.* **42** 3248–56